Effect of Y Addition on Microstructure and Mechanical Properties of Friction Stir Welded ZK60 Alloy

G.M. Xie[1,2)†], Z.Y. Ma[2)†] and L. Geng[1)]

1) School of Materials Science and Engineering, Harbin Institute of Technology, Harbin 150001, China
2) Shenyang National Laboratory for Materials Science, Institute of Metal Research, Chinese Academy of Sciences, Shenyang 110016, China

6 mm thick ZK60 and ZK60-Y alloy plates were successfully friction stir welded (FSW) at a tool rotation rate of 1200 r/min and a traverse speed of 100 mm/min. FSW resulted in the dissolution of $MgZn_2$ particles in the ZK60 and the breakup and dispersion of W-phase ($Mg_3Zn_3Y_2$) particles in the ZK60-Y alloy, thereby leading to a decrease in the hardness of the nugget zone (NZ) for the ZK60 alloy and an increase in the hardness of the NZ for the ZK60-Y alloy, respectively. While two FSW joints exhibited similar joint efficiency (87%–89% of ultimate tensile strengths of the parent materials), the yield strength of the FSW ZK60-Y joint was substantially higher than that of the FSW ZK60 joint. The fracture occurred in the NZ and the heat affected zone for the ZK60 and ZK60-Y joints, respectively, which were consistent with the lowest hardness distribution of the welded joints.

KEY WORDS: Friction stir welding; Magnesium; Microstructure; Mechanical properties

1. Introduction

Magnesium alloys exhibit lower density, higher specific strength, and good damping capacity than aluminum alloys[1,2]. Therefore, they are widely applied as structural parts in automotive and aerospace industries. Among the magnesium alloys, while the Mg-Al alloys (AZ and AM system magnesium alloys) have been widely applied, the ZK60 alloy with higher strength was developed. However, the thermal stability of the ZK60 alloy is poor. The additions of rare earth element Y into the ZK60 alloy can remarkably improve mechanical properties at high temperature. Therefore, the ZK60-Y alloys have attracted considerable research interests in recent years. Because the welding process is a thermal working process, the addition of rare earth element Y might change the weldability of the ZK60 alloy.

For the welded joints of the magnesium alloys produced by using conventional fusion welding, there are large deformation and residual stress, and welding defects such as hot crack, slag and porosity[3]. Friction stir welding (FSW), invented by The Welding Institute of the UK in 1991, is an energy-efficient, environment-friendly and versatile jointing technique that has proved to be one of the most significant achievements in the field of joining aluminum and magnesium alloys[4]. Therefore, the welding defects in the conventional fusion welds were not observed in the FSW joints due to the solid state process[5]. While the researches on the FSW magnesium alloys mainly focused on the Mg-Al system alloys[6–12], investigations into the FSW of Mg-Zn system alloys are relatively limited[13,14]. The present authors[13,14] have reported FSW studies of the ZK60 and ZK60-Y alloys. It was indicated that defect-free FSW joints of the ZK60 and ZK60-0.6Y alloys could be successfully achieved at a tool rotation rate of 800 r/min and a

traverse speed of 100 mm/min. However, because the welding was conducted by using differently-sized tool shoulders, it is hard to evaluate the effects of the addition of rare earth element Y on the weldability and joint properties of the ZK60 alloy.

In this paper, the extruded ZK60 and rolled ZK60-1.1Y plates with similar mechanical properties were subjected to FSW at a high rotation rate of 1200 r/min. The effects of Y addition on the microstructural evolution and mechanical properties of the welds were examined.

2. Experimental

Extruded ZK60 alloy and rolled ZK60-Y alloy with a composition of 6.0Zn-0.6Zr and 6.0Zn-0.6Zr-1.1Y (in wt pct), respectively, were used for this study. The plates 300 mm in length, 70 mm in width and 6 mm in thickness were machined from the extruded and rolled samples and welded at a rotation rate of 1200 r/min and a traverse speed of 100 mm/min along the extrusion/rolling direction using a gantry FSW machine. A tool with a shoulder 20 mm in diameter and a cylindrical threaded pin 6 mm in diameter and 5.7 mm in length was used. The tilt angle for all welds was maintained at 2.5° and the plunged depth was controlled at ∼0.2 mm.

The FSW samples were cross-sectioned perpendicular to the welding direction, polished and then etched with a solution of 90 ml ethanol, 10 ml distilled water, 5 ml acetic acid and 5 g picric acid. Microstructural features were characterized by optical microscopy (OM), scanning electron microscopy (SEM), and X-ray diffraction (XRD). Grain sizes were measured by the mean linear intercept method. The microhardness of the welded joints was measured along the mid-thickness of the plates with 500 g load for 10 s by using a LECO-LM247AT type Vickers-hardness machine. The transverse tensile specimens with a gauge length of 40 mm and a width of 10 mm were machined perpendicular to the FSW direction.

† Corresponding author. Ph.D.; Tel./Fax.: +86-24-83978908; E-mail address: gmxiehit@yahoo.com (G.M. Xie) and zyma@imr.ac.cn (Z.Y. Ma).
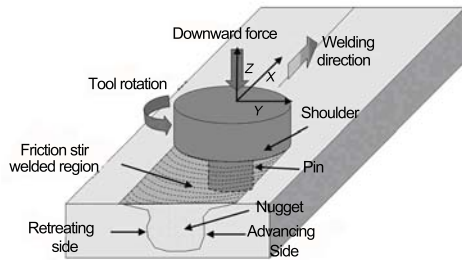
Fig. 1 Schematic drawing of friction stir welding[15]

The tensile test was carried out by using a Zwick-Roll-type testing machine at a strain rate of 4.2×10^{-4} s^{-1}.

3. Results and Discussion

Figure 1 is a schematic drawing of friction stir welding[5]. A non-consumable rotating tool with a specially designed pin and shoulder is inserted into the abutting edges of plates to be joined and traversed along the line of joint, producing a FSW joint. The cross-sectional macrographs of the FSW ZK60 and ZK60-Y joints are presented in Fig. 2. No welding defect was detected in these two joints, indicating that the sound FSW ZK60 and ZK60-Y joints could be achieved under the investigated welding parameter (rotation rate of 1200 r/min and traverse speed of 100 mm/min). Four microstructural zones were identified in the FSW ZK60 and ZK60-Y joints, *i.e.* the nugget zone (NZ), thermomechanical affected zone (TMAZ), heat-affected zone (HAZ), and parent material (PM). Figure 2 shows that the NZs of the FSW ZK60 and ZK60-Y joints exhibited similar basin shaped profiles, and the boundary between the NZ and TMAZ was clearer on the advancing side. Similarly, Gharacheh *et al.*[12] noted that a basin shaped NZ was obtained in a FSW AZ31 joint. The present authors[13,14] have reported that the typical basin shaped NZs were observed in the FSW ZK60 and ZK60-0.6Y joints at different welding conditions.

Figure 3 shows the microstructures of the PM and NZ of the ZK60 and ZK60-Y. The PMs of both ZK60 and ZK60-Y exhibited the heterogonous deformed grains (Fig. 3(a) and (c)). Besides, there were a certain amount of coarse second-phase particles in the ZK60-Y. The microstructures of the NZs of the FSW ZK60 and ZK60-Y joints were characterized by the fine and equiaxed recrystallized grains (Fig. 3(b) and (d)), indicating the occurrence of dynamic recrystallization due to intense plastic deformation and thermal exposure during FSW. Furthermore, the distribution of the second-phase particles in the NZ of the FSW ZK60-Y joint was improved compared to the PM. The average grain sizes in the NZs of the FSW ZK60 and ZK60-Y joints were determined to be 8.5 and 6.7 μm, respectively. Clearly, the average grain
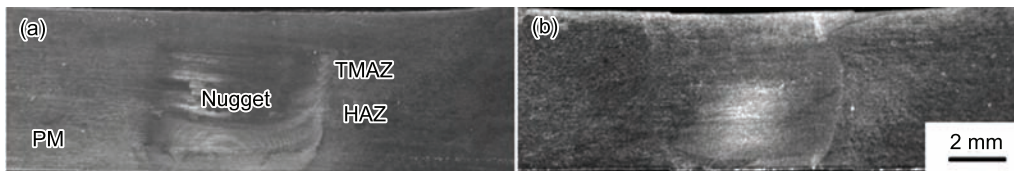
Fig. 2 Cross-section macrographs of FSW joints: (a) ZK60 and (b) ZK60-Y (the advancing side is on the right)
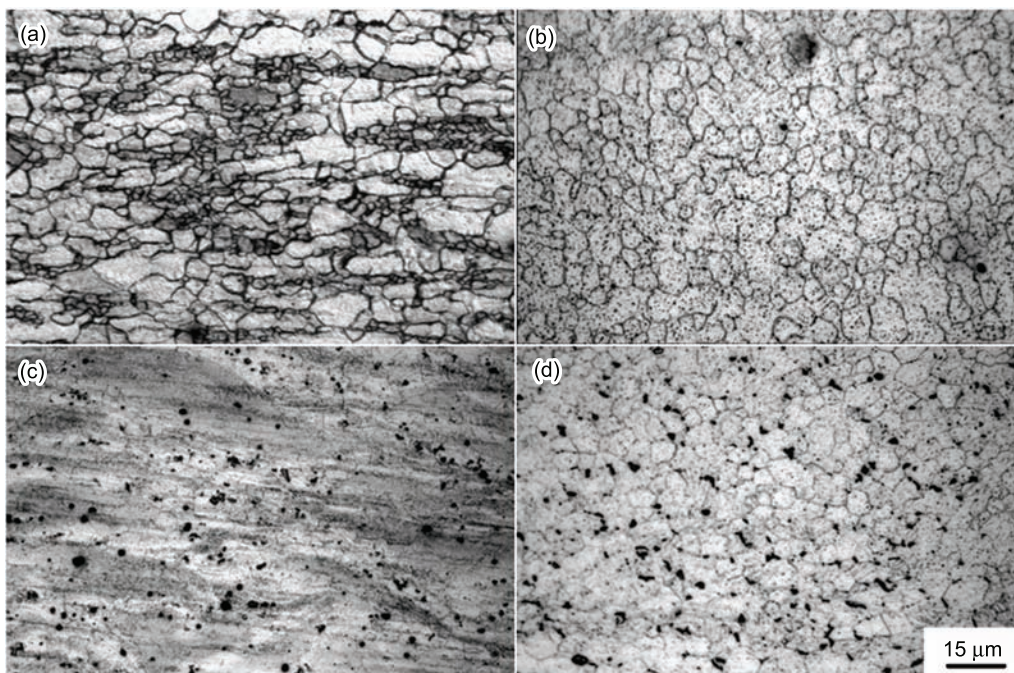
Fig. 3 Optical micrographs showing grain microstructure: (a) extruded ZK60, (b) NZ of FSW ZK60, (c) rolled ZK60-Y, and (d) NZ of FSW ZK60-Y
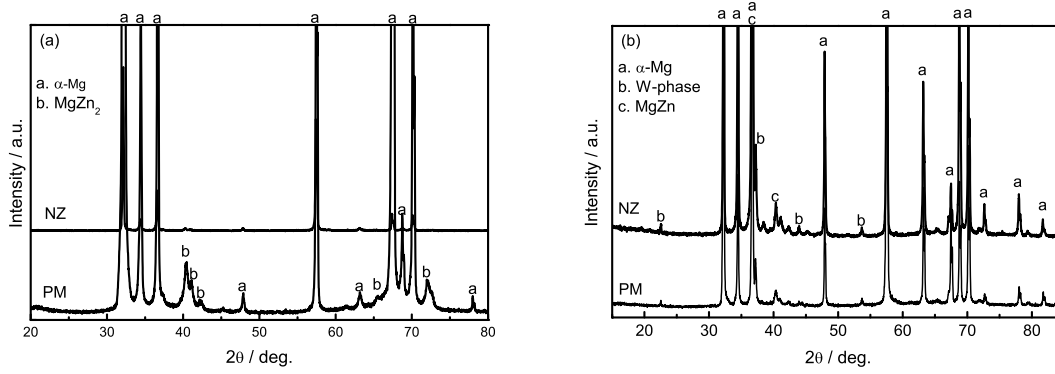
Fig. 4 XRD patterns of FSW joints: (a) ZK60 and (b) ZK60-Y
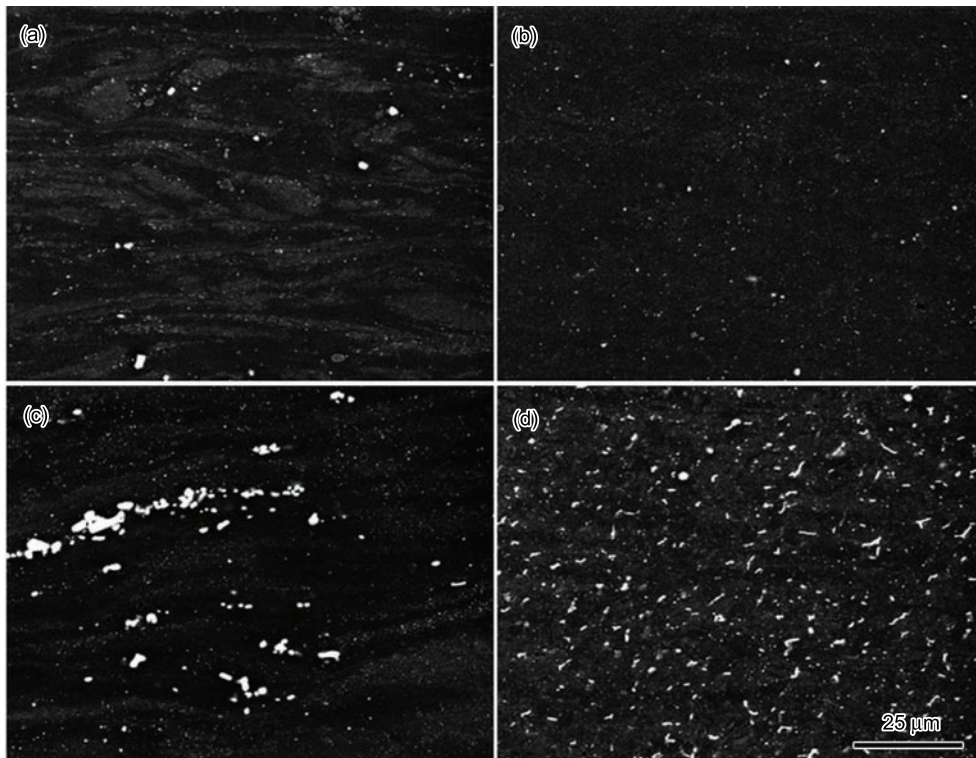
Fig. 5 SEM images showing second-phase particles: (a) extruded ZK60, (b) NZ of FSW ZK60, (c) rolled ZK60-Y, and (d) NZ of FSW ZK60-Y

size in the NZ of the FSW ZK60-Y joint is smaller than that of the FSW ZK60 joint. This is attributed to the existence of fine and homogeneous second-phase particles with excellent thermal stability. These particles impeded the growth of the recrystallized grains in the NZ of the ZK60-Y effectively. Park et al.[9] reported that 6.3 mm thick wrought AZ61 plate was successfully friction stir welded at 1220 r/min and 90 mm/min, and the average grain size in the NZ was 14 μm. This indicates that under similar plate thickness and welding parameter, the average grain size in the NZ of the FSW AZ61 is remarkably larger than that of the FSW ZK60 and ZK60-Y. This is because the Al12Mg17 phase in the AZ61 is not stable at high temperature. Therefore, the growth of the recrystallized grains during FSW could not be effectively inhibited. However, the addition of Y and Zr can effectively impede the growth of the recrystallized grains in the ZK60-Y and ZK60 alloys during FSW.

Figure 4 shows the XRD patterns of the PM and NZ for both ZK60 and ZK60-Y. While the diffraction peaks of α-Mg and MgZn$_2$ phase were detected in the PM of the ZK60, the diffraction peak of the MgZn$_2$ phase almost disappeared in the NZ of the ZK60 weld (Fig. 4(a)), indicating that most of the MgZn$_2$ phase was dissolved during FSW. For the PM of the ZK60-Y, the diffraction peaks of α-Mg, W-phase (Mg$_3$Zn$_3$Y$_2$), and MgZn phase were observed. After FSW, the diffraction peaks of the W-phase were still detected (Fig. 4(b)), indicating that the W-phase was thermally stable during the FSW thermal cycle. Clearly, the addition of rare earth Y element improved the thermal stability of the ZK60. Based on above results, it can be concluded that the temperature rise during FSW was higher than the dissolution temperature of the MgZn$_2$ phase, but lower than the eutectic temperature (510°C) of the W-phase.

Figure 5 shows SEM images of the PM and NZ for
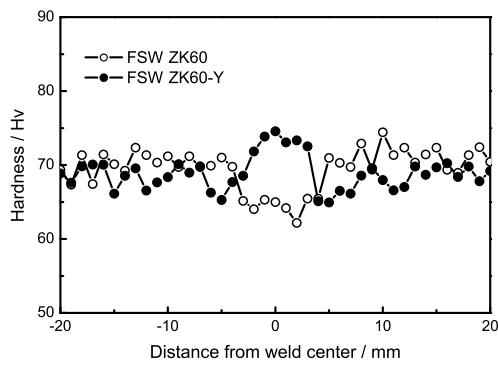
Fig. 6 Hardness profiles in cross-section of FSW ZK60 and ZK60-Y joints
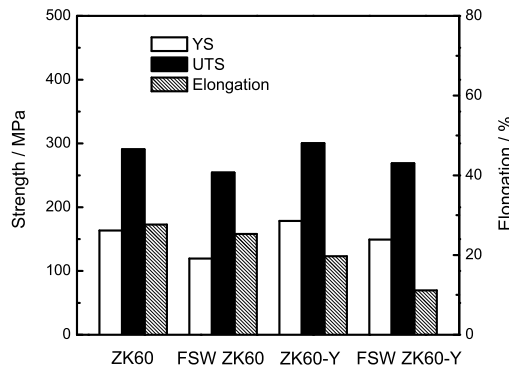
Fig. 7 Transverse tensile properties of PMs and welds of ZK60 and ZK60-Y

the ZK60 and ZK60-Y. During the hot extrusion of the ZK60, most of the MgZn$_2$ precipitates were dissolved into the magnesium matrix. Therefore, only a small amount of the MgZn$_2$ precipitates were observed in the as-extruded PM (Fig. 5(a)). FSW resulted in the breakup and further dissolution of the precipitates due to thermal exposure and intense plastic deformation. Thus, the amount and size of the precipitates in the NZ of the FSW ZK60 were significantly reduced (Fig. 5(b)), which is consistent with the XRD result (Fig. 4(a)). Clearly, under both as-extruded and as-welded conditions, fast cooling from the extrusion and FSW temperatures retained most of Zn in solution. For the ZK60-Y, after the hot rolling, the coarse W-phase particles in the as-cast ZK60-Y were broken up and distributed along the rolling direction. However, the size of the W-phase was still large and its distribution was non-homogeneous (Fig. 5(c)). In the NZ of the FSW ZK60-Y joint, significantly refined W-phase particles were homogeneously distributed in the magnesium matrix (Fig. 5(d)). This is attributed to significant breaking and dispersion effect of the threaded pin during FSW.

Figure 6 shows the hardness profiles along the centerline of the plates on the cross-section of the FSW ZK60 and ZK60-Y joints. The hardness values of the extruded ZK60 are slightly higher than those of the rolled ZK60-Y. Because the ZK60 is a precipitation-strengthened magnesium alloy, the hardness of the alloy is mainly governed by the precipitates. Fine MgZn$_2$ precipitates can increase the hardness of the ZK60. After Y addition into the ZK60, the phase composition of the ZK60-Y changed significantly com-
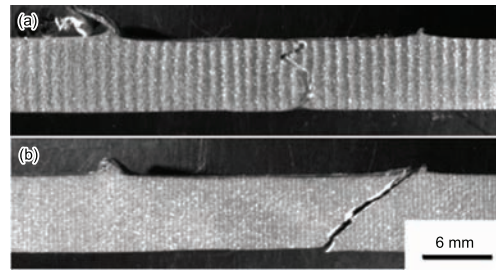
Fig. 8 Failed FSW ZK60 (a) and ZK60-Y (b) joints

pared to that of the ZK60. It was indicated that the MgZn$_2$ precipitates were replaced by the coarse W-phase particles. Ishikawa et al.[15] suggested that coarse eutectic Al12Mg17 phase hardly contributed to the average hardness value of the Mg-Al system alloys with a high Al content. Similarly, the coarse W-phase in the rolled ZK60-Y alloy hardly increased the average hardness of the material. Therefore, the hardness of the extruded ZK60 is higher than that of the rolled ZK60-Y. After FSW, the hardness values within the NZ of the ZK60 are lower than those of the PM due to the dissolution of the MgZn$_2$ precipitates, and the NZ is the lowest hardness zone. For the NZ of the FSW ZK60-Y joint, the coarse W-phase particles with high thermal stability were broken and dispersed. Therefore, the fine and homogeneous W-phase particle resulted in the enhancement in the hardness within the NZ of the FSW ZK60-Y joint. The lowest hardness zone was observed in the HAZ. This is attributed to annealing softening in the HAZ during the FSW thermal cycle. Therefore, the addition of Y element changed the hardness profile of the FSW ZK60 joint.

The transverse tensile properties of the FSW ZK60 and ZK60-Y joints are shown in Fig. 7. Compared to the PMs, the FSW ZK60 and ZK60-Y joints exhibited decreased mechanical properties. The tensile strength of the FSW ZK60-Y joint was higher than that of the FSW ZK60 joint, and specially, its yield strength was remarkably higher than that of the FSW ZK60 joint. For the FSW ZK60 and ZK60-Y joints, the fractures occurred in the NZ and HAZ (Fig. 8), respectively, which were consistent with the lowest hardness distribution of the welds (Fig. 6). In this case, the transverse tensile strengths of the FSW ZK60 and ZK60-Y joints are the strengths of the NZ and HAZ. The ZK60 is a precipitate-strengthened magnesium alloy, therefore, the dissolution of the precipitates in the NZ would result in remarkable decrease of the strength. After Y addition, fine and dispersed W-phase caused increasing of tensile strength in the NZ of ZK60-Y alloy, and the lowest strength zone located in the HAZ due to annealing softening.

However, the elongation of the FSW ZK60 joint is significantly higher than that of the FSW ZK60-Y. This is because the width of the NZ of the FSW ZK60 joint was larger than that of the HAZ of the FSW ZK60-Y joint, resulting in the occurrence of more uniform plastic deformation in the FSW ZK60 joint.

The yield ratios (YS/UTS) of the as-extruded and as-welded ZK60 are 0.56 and 0.46, indicating the remarkable decrease in the yield ratio of the ZK60. The yield ratios of the as-rolled and as-welded ZK60-Y are 0.59 and 0.55, respectively. This implied that yield

ratio of the ZK60-Y decreased slightly. Park *et al.*[9] reported that although the UTS of FSW AZ61 joint reached 94%, the yield ratios of the PM and welded joint were 0.55 and 0.37, respectively. This indicated that the yield ratio of the FSW joint was significantly lower than that of the PM for the AZ system magnesium alloys. By comparison, the FSW ZK60 and ZK60-Y joints exhibited higher yield ratio, in particular, the yield ratio of the FSW ZK60-Y was close to that of the PM.

4. Conclusions

(1) At a rotation rate of 1200 r/min and a traverse speed of 100 mm/min, sound FSW ZK60 and ZK60-Y joints 6 mm in thickness were achieved.

(2) The Y addition resulted in grain refinement in the NZ of the ZK60.

(3) For the ZK60, the hardness of the NZ was lower than that of the PM, and the lowest hardness values of the welded joint appeared in the NZ. After Y addition, the hardness of the NZ was higher than that of the PM with the HAZ being the lowest hardness zone.

(4) The UTS of the FSW ZK60 and ZK60-Y joints reached 87% and 89% of their PMs, respectively. After Y addition, the yield ratio (0.55) of the FSW ZK60-Y joint was significantly higher than that (0.46) of the FSW ZK60 joint.

REFERENCES

[1] M.M. Avedesian and H. Baker (Eds.): *Magnesium and Magnesium Alloys,* ASM, USA, 1999.

[2] I.J. Polmear: *Light Alloys,* 3rd edn., Arnold, London, 1995.

[3] Welding Handbook, China Machine Press, Bejing, 1992, **2**, 469.

[4] W.M. Thomas, E.D. Nicholas, J.C. Needham, M.G. Murch, P. Templesmith and C.J. Dawes: G.B. Patent: No. 9125978, 8, 1991.

[5] R.S. Mishra and Z.Y. Ma: *Mater. Sci. Eng. R,* 2005, **50**, 1.

[6] K. Nakata, S. Inoki, Y. Nagano, T. Hashimoto, S. Johgan and M. Ushio: *Proceedings of the third International Symposium on Friction Stir Welding,* Kobe, Japan, September 27-28, 2001.

[7] W.B. Lee, Y.M. Yeo and S.B. Jung: *Mater. Sci. Technol.,* 2003, **19**, 785.

[8] W.B. Lee, J.W. Kim, Y.M. Yeon and S.B. Jung: *Mater. Trans.,* 2003, **44**, 917.

[9] S.H.C. Park, Y.S. Sato and H. Kokawa: *Scripta Mater.* 2003, **49**, 161.

[10] J.A. Esparza, W.C. Davis and L.E. Murr: *J. Mater. Sci.,* 2003, **38**, 941.

[11] S.H.C. Park, Y.S. Sato and H. Kokawa: *J. Mater. Sci.,* 2003, **38**, 4379.

[12] M.A. Gharacheh, A.H. Kokabi, G.H. Daneshi, B. Shalchi and R. Sarrafi: *Int. J. Mach. Tool Manuf.,* 2006, **46**, 1983.

[13] G.M. Xie, Z.Y. Ma, L. Geng and R.S. Chen: *Mater. Sci. Eng. A,* 2007, **471**, 63.

[14] G.M. Xie, Z.Y. Ma and L. Geng: *Mater. Sci. Eng. A,* 2007, **486**, 49.

[15] K. Ishikawa, Y. Kobayashi, T. Kaneko and T. Shibusawa: *J. Jpn. Inst. Met.,* 1997, **61**, 1031.